


Research Paper

Axial and appendicular skeletal transformations, ligament alterations, and motor neuron loss in *Hoxc10* mutants

Sirrka Liisa Hostikka, Jun Gong, and Ellen M. Carpenter 

Department of Psychiatry and Biobehavioral Science, UCLA School of Medicine, Los Angeles, CA 90095, USA

 Correspondence to: Ellen M. Carpenter, Ph.D., Dept. of Psychiatry and Biobehavioral Science, UCLA School of Medicine, 635 Charles E Young Dr. South, NRB 303, Los Angeles, CA 90095. (310) 206-3404, (310) 206-5050 (fax), ecarpenter@mednet.ucla.edu

Received: 2009.03.12; Accepted: 2009.05.20; Published: 2009.06.03

Abstract

Vertebrate *Hox* genes regulate many aspects of embryonic body plan development and patterning. In particular, *Hox* genes have been shown to regulate regional patterning of the axial and appendicular skeleton and of the central nervous system. We have identified patterning defects resulting from the targeted mutation of *Hoxc10*, a member of the *Hox10* paralogous family. *Hoxc10* mutant mice have skeletal transformations in thoracic, lumbar, and sacral vertebrae and in the pelvis, along with alterations in the bones and ligaments of the hindlimbs. These results suggest that *Hoxc10*, along with other members of the *Hox10* paralogous gene family, regulates vertebral identity at the transition from thoracic to lumbar and lumbar to sacral regions. Our results also suggest a general role for *Hoxc10* in regulating chondrogenesis and osteogenesis in the hindlimb, along with a specific role in shaping femoral architecture. In addition, mutant mice have a reduction in lumbar motor neurons and a change in locomotor behavior. These results suggest a role for *Hoxc10* in generating or maintaining the normal complement of lumbar motor neurons.

Key words: *Hox* gene, vertebral column, hindlimb, motor neuron, patterning, locomotor behavior

Introduction

The *Hox* genes encode evolutionarily conserved transcription factors with *Antennapedia* class homeodomains. Mammals have 39 *Hox* genes in four conserved clusters, *HoxA*, *B*, *C*, and *D*, each located on a different chromosome. The clusters have been divided into 13 paralogous groups according to sequence similarities and position within the complex [1]. The *Hox* genes are expressed in a temporal and spatial order from 3' paralogous group 1 activated the earliest and with the most rostral limit of expression to 5' paralogous group 13 activated last and most posterior [2].

Vertebrate *Hox* genes have broad expression domains in developing embryos encompassing the paraxial mesoderm and neural tube, with more 5' *AbdB*-related *Hox* genes also expressed in the devel-

oping limbs. A large number of studies have examined the contributions of these genes to embryonic body plan development and patterning. These studies have shown that *Hox* genes can play roles in patterning the axial and appendicular skeleton, the nervous system, and the urogenital system [3-9]. Most of the *Hox* genes have been shown to regulate aspects of axial skeletal patterning, with mutations causing homeotic transformations of the vertebrae. These studies have suggested that *Hox* genes are particularly important in defining the regions of the axial skeleton and regulating the identity of the vertebrae found in these different regions.

The vertebrate axial skeleton is composed of cervical, thoracic, lumbar, sacral and caudal regions, with vertebrae in each region having a characteristic

shape and function. In C57Bl/6 mice, there are 30 precaudal vertebrae distributed into the four regions. There are seven cervical vertebrae, thirteen thoracic vertebrae, six lumbar vertebrae, and four sacral vertebrae [10-12]. Mutations in *Hox* genes typically do not affect the total number of precaudal vertebrae, but do affect the distribution of vertebrae in the different regions. Members of the *Hox5* and *Hox6* paralogous groups appear to regulate the identity of cervical and thoracic vertebrae, members of the *Hox9* and *Hox10* families regulate the thoracic and lumbar vertebrae, and members of the *Hox10* and *Hox11* families regulate lumbar and sacral identities [13]. Redundancy between members of paralogous gene families is also evident; in combinatorial mutants that eliminate the function of two or more paralogous genes synergistic phenotypes are always observed [8, 13-16]).

The *Hox10* gene family, comprised of three genes, *Hoxa10*, *Hoxc10*, and *Hoxd10*, is collectively required to pattern the lumbar vertebrae. Mutations in *Hoxa10* produce a partial or full transformation of the first lumbar vertebra into a thoracic phenotype, typified by the presence of an extra rib [8], while ectopic expression of *Hoxa10* in presomitic mesoderm deletes all ribs [17]. Combinatorial mutations in *Hoxa10* and *Hoxd10* also produce additional ribs, indicative of lumbar to thoracic transformations, and show sacral to lumbar transformations [8]. Combined mutations in all three *Hox10* genes produce animals in which both lumbar and sacral vertebrae are transformed to a thoracic identity, with vertebrae at thoracic, lumbar, and sacral levels all appearing to have associated ribs [16].

Phenotypes in *Hox10* mutants are not restricted to the axial skeleton, however. *Hoxa10* mutants have urogenital phenotypes including cryptorchidism in males and homeotic transformations of the uterus in females [4, 18]. Both *Hoxa10* and *Hoxd10* mutants have hindlimb skeletal alterations [4, 5, 7, 19] and *Hoxd10* mice have discernible alterations in the central and peripheral nervous system providing hindlimb innervation [7-9, 20]. These observations suggest widespread contributions of the *Hox10* genes to embryonic patterning.

Despite substantial examination of *Hoxa10* and *Hoxd10* mutants alone and in combination, there are relatively few studies examining individual phenotypes in *Hoxc10* mutants. Combinatorial studies suggest that loss of *Hoxc10* contributes to axial skeletal phenotypes [16] and a recent study of the nervous system shows a disruption in lumbar motor pool identity in embryonic *Hoxc10/Hoxd10* double mutants [20]. In the current study, we examined skeletal and nervous system phenotypes resulting solely from

disruption of *Hoxc10*. Unlike *Hoxa10* and *Hoxd10* mutant mice, all *Hoxc10* mutant mice are viable and fertile. In homozygous mutant mice, skeletal transformations are observed in thoracic, lumbar, and sacral vertebrae and in the pelvis, as well as in the bones and ligaments of the hindlimb. Heterozygous mice show intermediate forms and penetrance of the axial skeletal phenotype, suggesting dosage dependence. In addition, the number of lumbar motor neurons is significantly reduced, resulting in significant changes in locomotor behavior.

Methods and materials

Construction of the targeting vector

A replacement targeting vector was constructed from 129Sv mouse genomic clones for the *Hoxc10* gene that were isolated from a CC1.2 embryonic stem (ES) cell-derived library [3, 21]. A 157 bp deletion flanked by P1fM1 and BamHI restriction sites was made in the second exon to remove the last 50 amino acids of the homeodomain, and the deleted sequence was replaced with an in-frame fusion of a *lacZ* gene with SV40 polyadenylation signal [22] followed by a polII promoter-driven *neomycin resistance* gene cassette KT3NP4 (*neo^R*, [23]; see Figure 1). The *lacZ/neo^R* sequences were flanked by 8.7 and 3.1 kb of 5' and 3' genomic sequence, respectively, resulting in 11.8 kb of total homology. The replacement sequence was assembled in the KSTK9XbaTK2-2 *thymidine kinase* gene plasmid vector [24] resulting in a 26.3 kb targeting vector that was linearized for electroporation by digestion with PvuII. Junctions of individually cloned pieces were verified by sequencing across the restriction sites and into the *neo^R* and *LacZ* genes.

Creation and genotypic analysis of mutant mice

The targeting vector was electroporated into CC1.2 ES cells and the cells were subjected to positive-negative selection and cloned as previously described [25]. The cell lines were analyzed for targeting events with the following probes: pro 5, a 1.1 kb EcoRI - BamHI 5' flanking probe, pro 4, a 2.3 kb BglII - BamHI 3' flanking probe (see Fig. 1), and *neo^R* and *LacZ* specific internal probes. The primary screen was carried out with a BamHI digestion of DNA from each cell line probed with pro 4, which reveals a 6.5 kb wild-type and an 8.9 kb recombinant fragment. Positive cell lines were confirmed with a XhoI - SphI digest that results in a 18.5 kb wild-type and 13 kb recombinant band with pro 4, and 12.7 kb and 13 kb fragments with *neo^R* probe hybridization. The 5' flanking probe, pro 5, detects a 11.5 kb wild-type and 18.8 kb mutant fragment in *ScaI* digested DNA, the latter of which also hybridizes to *neo^R* probe. Pro 5

also shows a shift from a 25 kb wild-type to a 17 kb fragment in a MluI - SpeI digestion, which, in addition to a 12.3 kb fragment, is detectable with the *LacZ* probe. Full targeting and analysis strategy is provided in Supplemental Figure 1. Ten out of 106 cell lines had the desired targeting event. One of these also had a random integration detected as an unexpected additional band with internal probes; this line was subsequently discarded. Two of the correctly targeted cell lines were injected into blastocysts that were implanted into pseudopregnant females. The cell line 1d-8 produced 13 male chimeras. These were mated to C57Bl/6J females (Jackson Laboratory) and produced 249 offspring, one of which had the agouti coat color marker for germ-line transmission. Genotypic analysis of tail DNA isolated from this male proved that the mouse carried the targeted mutation, and it was mated to C57Bl/6J females to propagate the line. Ad-

ditional backcrosses were made to bring the line to a uniform C57Bl/6J background. Once the backcrossing was completed, the line was propagated by heterozygous intercrosses to generate mutants and wild-type littermates for further analysis.

Hoxc10 progeny were genotyped either by the original Southern analysis or by PCR. PCR was performed using the following primers: *Hoxc10* forward: 5'-AAGCTGCACCAAGGTCTTGGGTC-3'; *Hoxc10* reverse: 5' AATTGGAGGTCAGTTCCTCCGGATC 3' and *lacZ*-specific: 5'-CGCGCTCGAGATGTGCTGCAAGGCGATTAAG-3'. PCR cycle conditions were 35 seconds at 94°C, 15 seconds at 59°C, and 40 seconds at 72°C for 32 cycles. PCR bands were visualized on a 6% polyacrylamide or 1.5% Trevigel agarose gel (see Figure 1) and generated a WT band of 327 bp and a mutant band of 228 bp.

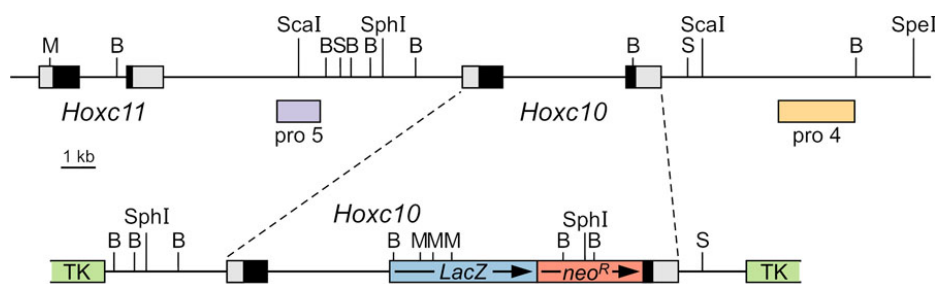


Figure 1. Generation of *Hoxc10* knockout allele. Schematic representations of the *Hoxc10* genomic region (top) and targeting vector (bottom). An in-frame fusion of *LacZ* and *neo^R* was inserted into the coding sequence (black shading) of *Hoxc10* exon 2. The position of 5' and 3' flanking probes pro5 (lavender) and pro4 (yellow) used for Southern analysis are indicated in association with the genomic region schematic. The engineered sequence was flanked by thymidine kinase genes (TK) in the assembled targeting vector. Restriction sites for BamH I (B), Mlu I (M), Sal I (S), Sca I, Spe I, and Sph I are indicated.

Tissue and skeletal analysis

Newborn and adult mice were asphyxiated with CO₂ and dissected tissues were fixed by immersion in Bouin's fixative or 4% paraformaldehyde for histological analysis. Specimens were embedded in paraffin and 10 µm serial sections were collected and stained with hematoxylin and eosin. Adults of all different genotypes were collected from littermates at 8 weeks (if not otherwise stated) for skeletal analysis and tissue collection. Skeleton preparations and X-gal staining were performed as described [7, 26]. Immunohistochemical labeling was carried out according to established protocols [27]. Anti-neurofilament antibodies (2H3) and anti-islet-1 antibodies (2D6) were obtained from the Developmental Studies Hybridoma Bank.

Rotarod analysis

Locomotor behavior was assessed using a rotarod. Three month old sex-matched littermates were

positioned on a rotarod apparatus rotating at 5 rpm. Once all mice were in position, the rotation was accelerated from 5 to 60 rpm over 180 sec and the rpm at fall recorded. Four trials were performed for each animal and the average rpm at fall calculated for each genotype. Statistical analysis of the results was performed using a Student's 1-tailed t-test assuming unequal variance. Initial analysis was performed separately on male and female mice, but as no differences in rotarod behavior were observed between males and females of the same genotype, data from both sexes were aggregated for the final statistical analysis.

Cell counting

Motor neuron cell counts on newborn animals were performed as previously described [9]. Briefly, the position of the lumbar spinal segments was identified by screening serial histological sections for the position of the dorsal root entry zone and spinal

nerves. The first lumbar segment was identified as the segment that contained the rostral end of the lateral lumbar motor column; spinal segments were then counted caudally from this reference point with the midpoint between adjacent spinal nerves used as the boundary between adjacent segments. Once segmental position was defined, motor neurons were systematically counted. Lumbar motor neurons were identified by size and position in histological sections; only cell profiles possessing a complete nuclear membrane and at least one distinct nucleolus were counted to minimize double counting. Both medial motor column and lateral motor column motor neurons were counted. Motor neuron counting data was compiled in Microsoft Excel and subjected to statistical analysis using Student's two-sample t-tests assuming unequal variance.

Results

Hoxc10 mutant mice

The *Hoxc10* targeting vector was constructed such that most of the homeodomain sequence was replaced with an in-frame lacZ gene and a polymerase II promoter-driven *neo^R* cassette (Figure 1). This targeting strategy deletes all three alpha-helices of the homeodomain, producing a protein lacking the ability to bind to DNA. All possible genotypes were obtained in Mendelian ratios following heterozygous intercrosses, and *Hoxc10* mutant mice are viable and fertile. The embryonic expression pattern of the fusion protein, as detected by X-Gal staining, is nearly identical to the previously described mRNA expression pattern [21, 26]. β -galactosidase expression is evident in caudal regions of the embryo including the pre-vertebrae, spinal cord, genital tubercle, and kidney, as well as surrounding the cartilage condensations of the pelvis (Figure 2). Expression is also found in the proximal hindlimb, particularly in the perichondrium surrounding hyaline cartilage precursors of the tibia and femur (Figure 2C) and in the iliofemoral ligament (Figure 2D-F). β -galactosidase expression is also detected in the developing nervous system, with expression overlapping that of *Islet-1* in developing motor neurons in the lumbar spinal cord (Figure 2G,H). No overt behavioral phenotypes were observed, although with age, mutant mice show signs of hindlimb wasting and a high incidence of obesity. Both of these phenotypes are presumably caused by the abnormal iliofemoral ligament and the loss of motor neurons (described below), which may cause restricted mobility. In addition, 5 of 60 mutants examined had a single kidney.

Axial skeletal phenotypes

The lack of a functional *Hoxc10* homeobox causes several homeotic transformations in the axial skeleton (Table 1, Figures 3 and 4). Wild-type C57Bl/6 mice typically have 30 precaudal vertebrae, with the more caudal vertebrae organized in T13L6S4 pattern, with thirteen thoracic vertebrae, six lumbar vertebrae and four sacral vertebrae [10, 11]. Eighty percent of the wild-type mice examined in this study exhibited this pattern, with the remainder of the animals showing some mild variation in the shape of the L1, L6, or S1 segments; these types of variations are within the range of normal ([10]. *Hoxc10* mutant mice also have 30 precaudal vertebrae, but the patterning of the vertebral column is altered. Most *Hoxc10* mutant mice (33 of 34 examined) show a partial to complete transformation of the thirteenth thoracic vertebrae, precaudal vertebra 20 (PC20) into a lumbar identity, typified by the reduction or complete loss of the thirteenth rib. By definition, thoracic vertebrae are those vertebrae with attached ribs; hence loss of the thirteenth rib suggests a posterior transformation of the most caudal thoracic vertebra into a lumbar identity. The most caudal lumbar vertebra (PC25) often undergoes a similar transformation into a sacral (S1) identity (Figures 3 and 4). The sacrum in wild-type animals is typically comprised of four vertebrae. The first two vertebrae, S1 and S2, have butterfly-shaped, fused transverse processes. The next two sacral vertebrae, S3 and S4, have transverse processes that are not fused, with S3 having butterfly-shaped transverse processes and S4 having club-shaped transverse processes similar to those seen on more caudal vertebrae (Figures 2 and 3). In *Hoxc10* mutant animals, the fourth sacral vertebra (S3* in Figures 3 and 4) exhibits an intermediate shape between a normal S3 and S4, and there are usually five sacral-like vertebrae, three fused and two free. This suggests an anterior transformation of the first caudal vertebra into a sacral identity. This transformation restores the register of the vertebral column and thus there is no overall loss of precaudal vertebrae. In combination, these alterations produce a T12(T13/L1)L5S5 pattern in 94% of mutant mice. Heterozygous mice show several intermediate patterns, most commonly T13L5S5 (31.5%) or T12(T13/L1)L5S5 (38.9%), suggesting dosage compensation. The transitional vertebra, defined as the most anterior vertebra to show a lumbar rather than a thoracic articulation between the pre- and postzygapophyses [28 and references therein] is normally the tenth thoracic vertebra (T10), whereas in the homozygous *Hoxc10* mutants the transition occurs at the ninth thoracic vertebra (T9) (Figure 4).

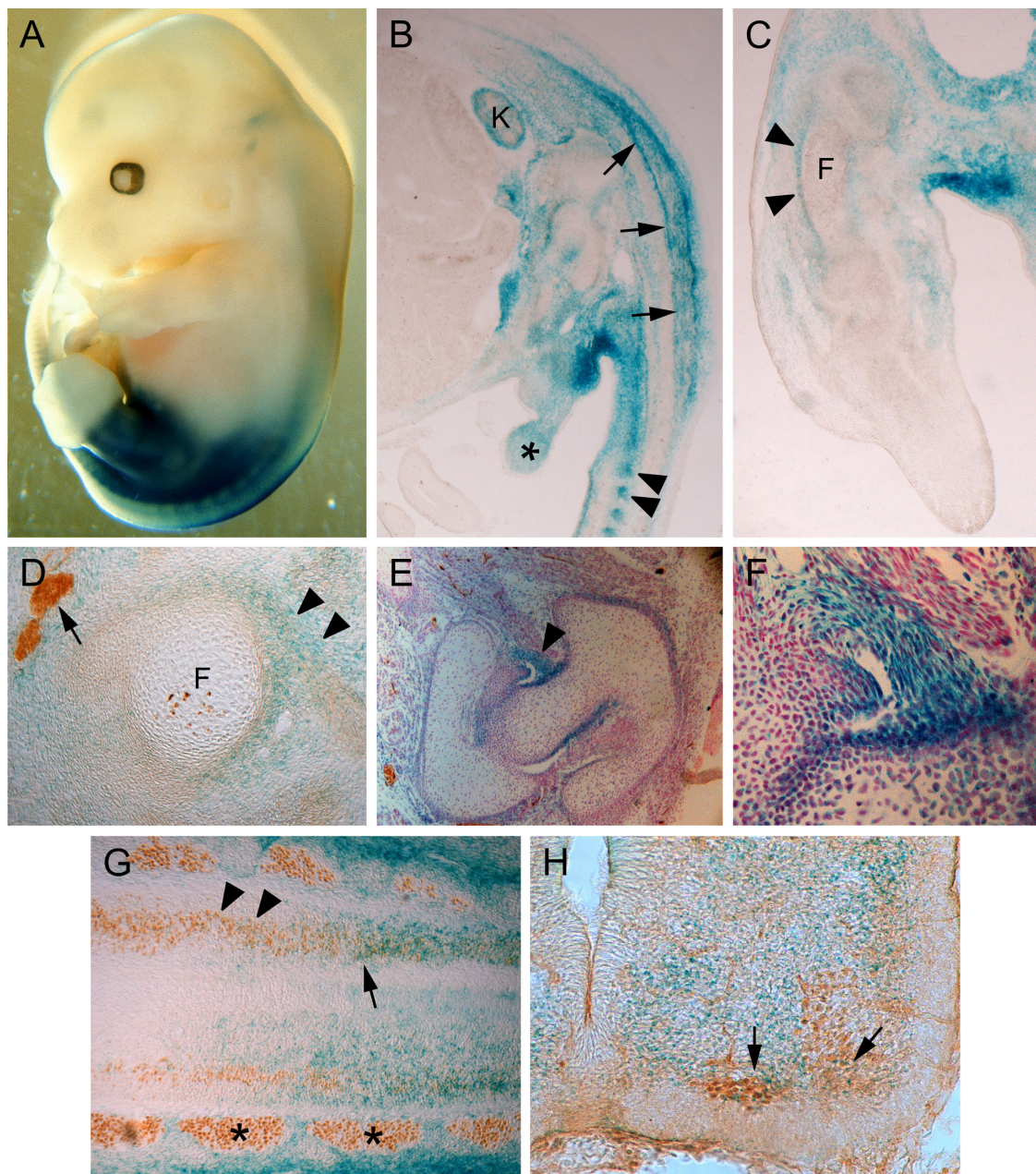


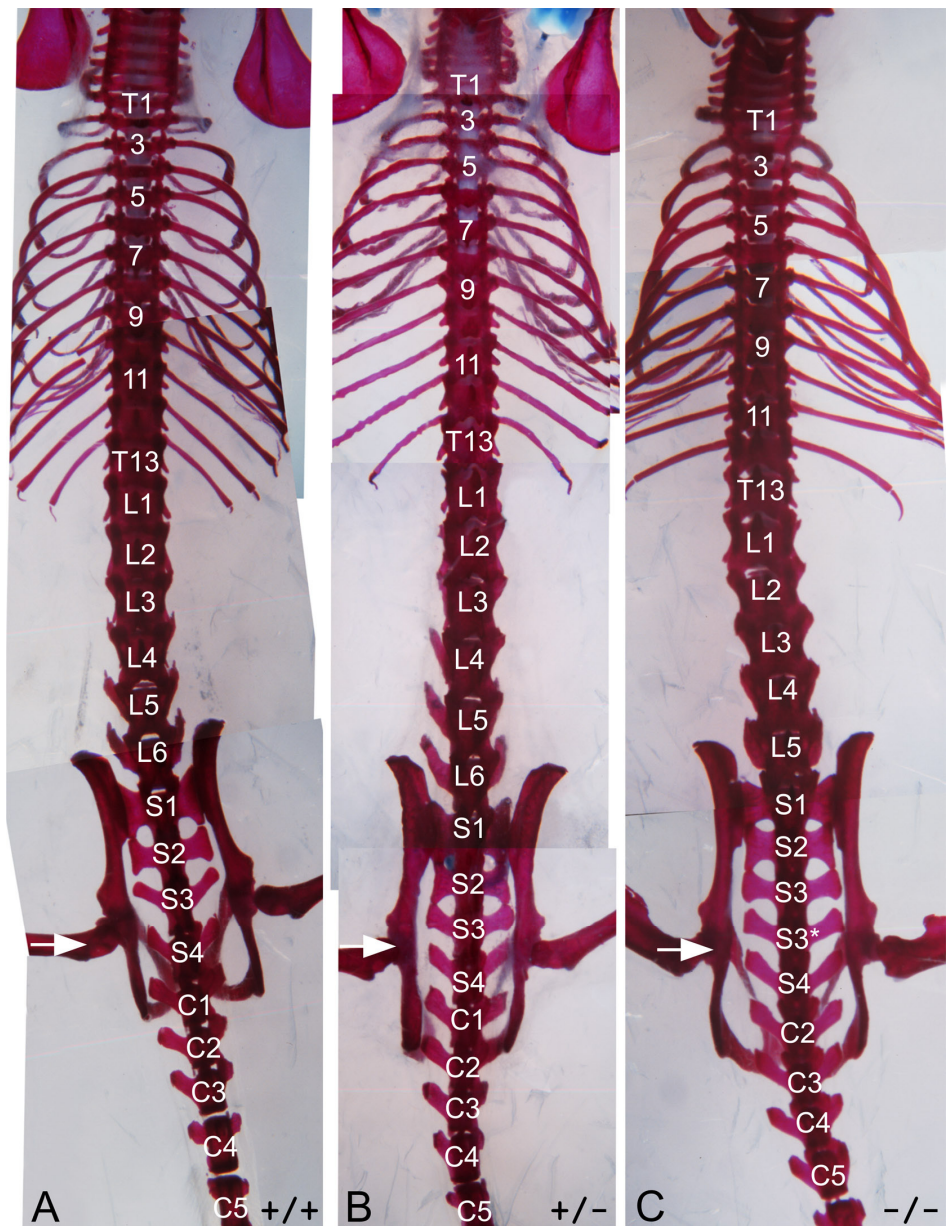
Figure 2: *Hoxc10* expression in developing mice. (A) Wholemount view of E13.5 *Hoxc10*^{+/-} embryo reacted with X-Gal for visualization of β -galactosidase expression. *Hoxc10* expression is confined to the posterior region of the embryo and to the proximal hindlimb. (B) Sagittal section through E13.5 embryo illustrating β -galactosidase expression in the spinal cord (arrows), caudal prevertebrae (arrowheads), kidney (K), and genital tubercle (*). (C) Longitudinal section through E13.5 hindlimb illustrating *Hoxc10* expression in the perichondrium surrounding the cartilage condensations of the femur (F) and tibia (T). (D) Transverse section through an E13.5 hindlimb. *Hoxc10* is expressed in the developing iliofemoral ligament (arrowheads) attaching to the femur (F). Arrow indicates the femoral nerve labeled with anti-neurofilament antibody. (E) Section through the developing hip joint in a newborn animal. *Hoxc10* is expressed in the iliofemoral ligament (arrowhead, higher magnification in F). Section is counterstained with nuclear fast red. (G) *Hoxc10* is expressed in the lumbar spinal cord (arrow) overlapping regions of islet-1 expression (brown reaction product). At more rostral levels, islet-1-positive cells do not express *Hoxc10* (arrowheads). *, DRGs. (H) Transverse section through the spinal cord illustrating overlap of *Hoxc10* and Islet-1 expression in the lumbar motor column (arrows).

Table 1: Axial skeletal phenotypes of *Hoxc10* mutant mice and litter mates

Genotype	+/+	+/-	-/-
Vertebral pattern			
T13(T14/L1)L5S4	4.8% (1)		
T13L6S4	80.0% (17)	20.4% (11)	
T13L5(L6/S1)S4	9.5% (2)	7.4% (4)	2.9% (1)
T12(T13/L1)L5(L6/S1)S4		1.9% (1)	
T13L5S5	4.8% (1)	31.5% (17)	
T12(T13/L1)L5S5		38.9% (21)	94.0% (32)
T12L6S5			2.9% (1)
Transitional vertebra			
T10	100%	90.7%	
T9		9.3%	100%

Precaudal vertebral patterns are indicated as total number of vertebrae of thoracic, lumbar, and sacral vertebrae. Partially transformed vertebrae that share features of two types of vertebrae are indicated in parentheses. All animals examined had 30 precaudal vertebrae. The number of mice having each phenotype is indicated in parentheses.

Figure 3: *Hoxc10* axial skeletal phenotypes. Dorsal views of wild-type (A), heterozygous (B) and homozygous mutant (C) *Hoxc10* adult mouse skeletons. Vertebral identities are indicated on the panels and the white arrows show the position of the acetabulae. Asterisks indicate transformed vertebrae. T, thoracic, L, lumbar, S, sacral, C, caudal.



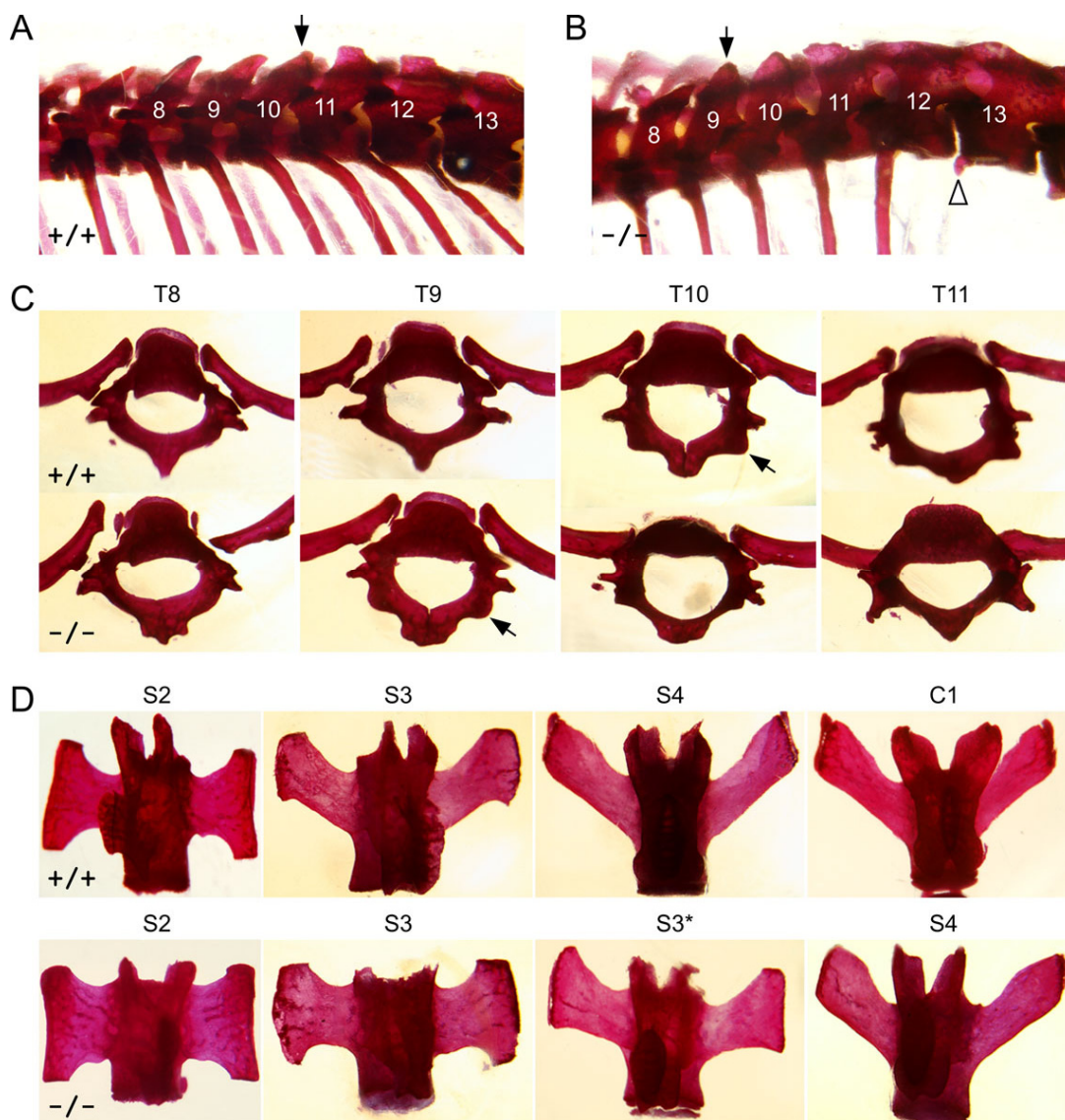


Figure 4: Vertebral phenotypes in *Hoxc10* mutants. Arrows in panels A and B illustrate the position of the transitional vertebra in wild-type and mutant animals, respectively. There is a rudimentary rib on the T13 vertebra (open arrowhead in B). Thoracic and sacral vertebral shapes are illustrated in panels C and D. The position of the costal facet, marked by arrows in C, denotes the transitional vertebra. Panel D illustrates the morphology of the sacral vertebrae. The transverse processes of the mutant S3* vertebra (bottom row) have an intermediate shape.

Pelvic bone phenotypes

The bones in the hip, the ilium, ischium and pubis, are constructed from independent condensations that grow together after birth. All three bones meet at the acetabulum, but the ischium and pubis also meet at the ventral edge of the pelvis. These two bones are angled 45° from each other on the anterior, acetabular end, and are connected by a cartilaginous bridge where they meet on the posterior side. This bridge undergoes calcification during puberty, and the pelvic apparatus is normally fully fused by eight weeks of age. In *Hoxc10* mutants, the cartilaginous bridge forms normally, but the calcification process is de-

layed, leaving a prominent seam or indentation on the posterior edge of the pelvis, dyssymphysis ischio-pubica. In all mutant adults the bones touch each other but even in the mildest cases, a seam is visible unlike in the controls (Figure 5A, B; Table 2). The C57Bl/6 background strain has been reported to have high incidence of dyssymphysis, especially in females [29, 30], however, somewhat newer reports have claimed only 30% incidence which was lost when C57Bl/6 mice were crossed to another strain [31]. To minimize differences attributable to genetic background, wild-type sibling controls were used for all experiments.

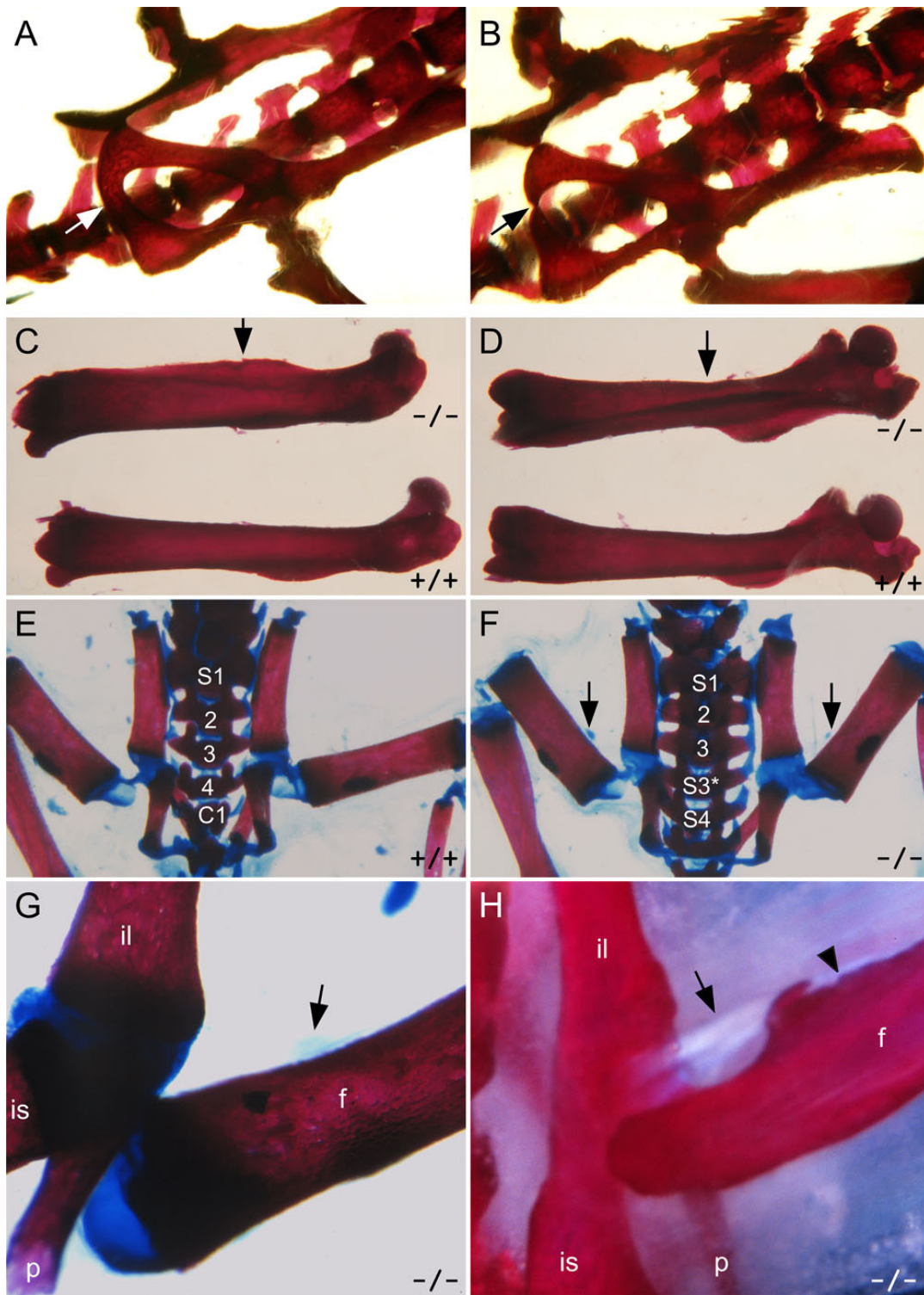


Figure 5: Pelvic girdle and hindlimb phenotypes in *Hoxc10* mutant mice. (A, B) Pelvic bones in adult wild-type and mutant mice. The fusion between the pubic and ischial bones is delayed, producing a noticeable seam (dyssymphysis ischio-pubica) in the mutant pelvic girdle (arrows). (C, D) Lateral (C) and anterior (D) views of the femur in mutant (upper) and wild-type (lower) mice. The position of an ectopic bony ridge along the anterior shaft of the mutant femur is indicated by arrows. (E, F, G) Alizarin red and alcian blue-stained skeletal preparations of newborn animals illustrate that the ectopic femoral ridge is not present, but that the cartilaginous condensation illustrating the attachment point of the abnormal iliofemoral ligament is visible in mutant animals (F, G, arrows). (H) Both the abnormal iliofemoral ligament (arrow) and ectopic femoral ridge are visible in adult mutant mice. f, femur, il, ilium, is, ischium, p, pubis.

Table 2: Appendicular skeletal phenotypes in adult *Hoxc10* mutant mice

Genotype		+/+	+/-	-/-
Pelvis	Open I/P*		4.0% (3)	67.6% (25)
	Visible seam	16.7% (5)	44.0% (33)	27.0% (10)
	Fused I/P	83.3% (25)	52.0% (39)	5.4% (2)
Femur	Prominent ridge			94.6% (35)
	Moderate ridge		1.3% (1)	5.4% (2)
	No ridge	100% (30)	98.7% (74)	

Skeletal analysis of mice at 8+ weeks of age. The number of mice having each phenotype is indicated in parentheses.

*open I/P= posterior complete dyssymphysis of ischium and pubis

The position of the pelvic girdle relative to the spinal column in general does not change in *Hoxc10* mutants. At embryonic days 12.5-14.5 (E12.5-14.5), the femoral condensation of the hindlimb buds form at the level of prevertebrae 25 - 26 in both mutants and the wild types. However, the acetabulum is adjacent to the boundary between the third and fourth sacral vertebrae (S3 and S4) in both newborn and adult wildtype mice, while it is seen at the level of the fourth and fifth sacral vertebrae (S3* and S4) in most mutants. However, in both WT and mutant animals, this positioning places the acetabulum at the level of the boundary between the PC29 and PC30 vertebrae. Thus, the overall position of the acetabulum does not change in *Hoxc10* mutant animals.

Hindlimb phenotypes

There are several alterations in hindlimbs and hip joints in *Hoxc10* mutants. During embryonic and early postnatal development, there are no visible skeletal defects in the hindlimbs. However, by four to six weeks postnatally, a bony ridge develops along the anterior longitudinal line of the shaft of the femur (Figure 5). A likely cause for the formation of this femoral ridge is the presence of an ectopic branch of the iliofemoral ligament. The iliofemoral ligament is a sheet-like structure on the anterior side of the femoral neck, acting as a part of the synovial capsule. Normally, the ligament joins the ilium anterior to the acetabulum of the hip joint to the intertrochanteric line of the femur. During development, this ligament expresses *Hoxc10* (Figure 2C-F). The ischiofemoral ligament connects the dorsal aspect of the ischium to the femoral neck. In the mutant, the ischiofemoral ligament is visibly weaker than in the wild-type mice, and attaches more dorsally to the medial side of the rim. The iliofemoral ligament, on the other hand, has two femoral connections in the mutants: one normal connection that attaches as a part of the synovial

capsule into the femoral neck and another that attaches onto the anterior shaft of the femur (Figures 5 and 6). This second ectopic branch attaches to and is part of the anterior femoral ridge. The point of attachment varies from just distal to the intertrochanteric line to halfway down the femur, likely affecting the extent of ridge calcification that varies between animals and progresses with age. This phenotypic attachment site variation likely drives the differences in the shapes of the femoral ridges of the mutants from prominent to moderate, reflecting additional stresses on the bone. The femoral ridges are found in all the mutants six weeks and older (Table 2). Histological study of the extra ligament shows an organized fibrillar structure, indicating no aberrant pathology (Figure 6C). Serial sections of newborns show the ligament attaching to the femoral shaft (Supplemental Figure 2), also seen in some newborn skeletal preparations as Alcian blue-stained material in the ridge area indicating cartilaginous material, likely sulfated proteoglycans, at the femoral end of the abnormal ligament (Figure 5F, G).

Histological studies of the hip joint reveals further age-related changes. In adult mutant mice, the articular hyaline cartilage of the femoral head is thinner than normal, and does not have well-organized maturation layers (Figure 7A, B). In most mutants, no epiphyseal line is found. Transverse sections of adult wild-type thighs show an oval femoral bone, whereas the mutant femur is almost triangular with the anterior ridge forming the tip (Figure 7C, D). The lateral and medial posterior lips are formed by the lesser trochanter and third trochanter on the proximal side continuing as medial and lateral supracondylar ridges distally by the knee. These structures form the two lips of the posterior femoral prominence, the linea aspera, which mice do not have as a distinguishable structure but which in several other mammals is a major posterior muscle attachment site. In mice, the equivalent muscles attach on an invisible line at the posterior, posteromedial and posterolateral positions of the oval bone. The posterior muscle attachment region cannot be found either in heterozygous or homozygous *Hoxc10* mutants.

Hindlimb musculature appeared relatively normal in *Hoxc10* mutant mice. Homozygous mutants have substantially shorter muscles on the medial side of the thigh compared to wild type, but the femur is also shorter. All muscles were found in their normal relative positions and their attachment sites were approximately normal on their femoral ends. The psoas muscle attaches to the lesser trochanter on the femur and to the ventral side of the lumbar vertebrae; how-

ever, a more anterior vertebral attachment in the mutant animals could not be ruled out. At weaning, the mutant and littermate hindlimbs are indistinguishable, but muscle wasting becomes apparent in older

mice. By 14 weeks of age total muscle mass is about 70% of normal by weight of dissected muscles.

Figure 6: Iliofemoral ligament phenotypes. (A, B) The iliofemoral ligament attaches to the acetabular rim of the ilium and the intertrochanteric line of the femur (arrows in A, B) in both wild type (A) and mutant (B) animals. In the *Hoxc10* mutant, there is an additional branch of the ligament to the anterior shaft of the femur (arrowhead in B). (C) Histologic section stained with hematoxylin and eosin showing that the mutant branch of the iliofemoral ligament is part of the synovial capsule surrounding the femoral head (h) and is directly attached to the bony part of the ectopic femoral ridge (r).

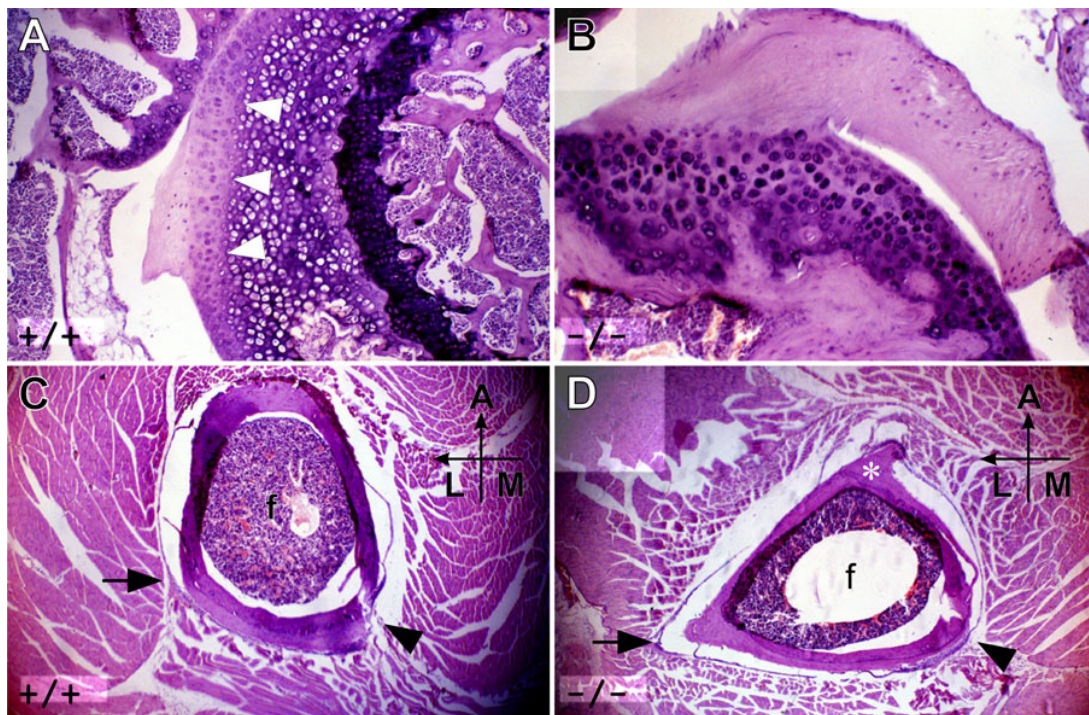
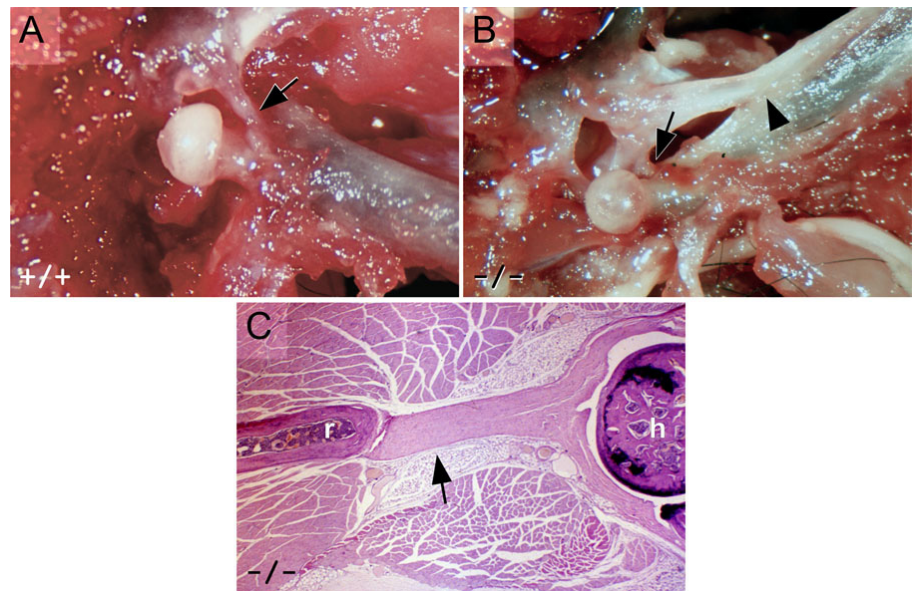


Figure 7: Femoral bone and cartilage structure in *Hoxc10* mutants. (A) A transverse histological section through the head of the femur. The epiphyseal line (arrowheads) is clearly visible surrounded by thick hyaline cartilage in a wild-type mouse. Several distinct cartilaginous layers, indicating different phases of maturation, are also evident. (B) *Hoxc10* mutant mice have reduced amounts of hyaline cartilage, no clear separation of bone and cartilage, and no visible epiphyseal line. Also missing is evidence of differences in cartilage maturity. Transverse sections through the shaft of the femur show that the wild-type femur is oval (C), whereas the mutant is more triangular (D) with an anterior ridge (D, asterisk) forming a tip. The lateral (arrow) and medial (arrowhead) supracondylar lines are marked and the anterior (A), lateral (L) and medial (M) orientation of the section is indicated.

Behavioral phenotypes

Initial open field observations suggested that there were no overt differences in locomotor behavior or motility in *Hoxc10* mutants. *Hoxc10* mutant mice had normal gaits and were able to grasp a pencil positioned along their ventral midline, a test of adduction. Open field behaviors were also normal, with mutant mice entering the same number of quadrants in an open field as wild-type mice. However, as concurrent observations suggested a significant loss of motor neurons in *Hoxc10* mutants (see below), we performed a rotarod analysis as a specific test of locomotor function. A total of 19 mutant and 13 wild-type three-month old animals were subjected to rotarod testing as described in the Methods and Materials. The average rpm at fall was 35.5 ± 11.8 for wild-type animals and 27.1 ± 9.1 for mutant animals (Figure 8). A one-tailed t-test, assuming unequal variance demonstrated that the results were significantly different, with $p < 0.001$.

Nervous system phenotypes

Initial analysis of peripheral nerve projection patterns in *Hoxc10* mutant embryos using anti-neurofilament antibody labeling suggested that there were no gross defects in the formation, appearance, and projection of spinal nerves in *Hoxc10* mu-

tant embryos. Motor and sensory projections into the developing hindlimb bud appeared normal as well (Figure 2). However, in light of alterations in motor neuron positioning in paralogous *Hox10* gene mutants [8, 9] we decided to examine these neurons more carefully in serial histological sections collected from newborn animals. Serial 10 μm sections were collected from three wild-type and three *Hoxc10* mutant animals. Lumbar segmental position was established as previously described [9] and the number of motor neurons in the medial and lateral motor columns (MMC and LMC, respectively) in the L1-L4 spinal segments was counted. All motor neuron populations showed substantial reductions in *Hoxc10* mutants (Figure 8). We further distinguished both medial and lateral components of the LMC; both components showed similar reductions in numbers of motor neurons. Despite the reduction in numbers of motor neurons, the distribution of these neurons appeared relatively unchanged, with MMC and LMC_M neurons showing a peak in their distribution in segment L2 and LMC_L neurons peaking in segments L3/L4. This suggests an absence of an anterior spinal segmental transformation, in contrast to results observed in *Hoxd10* mutants and *Hoxa10/Hoxd10* double mutants [7, 8]. These cell counts appear to reflect an absolute loss of motor neurons, as there is no evidence of compensation in one pool for losses in another.

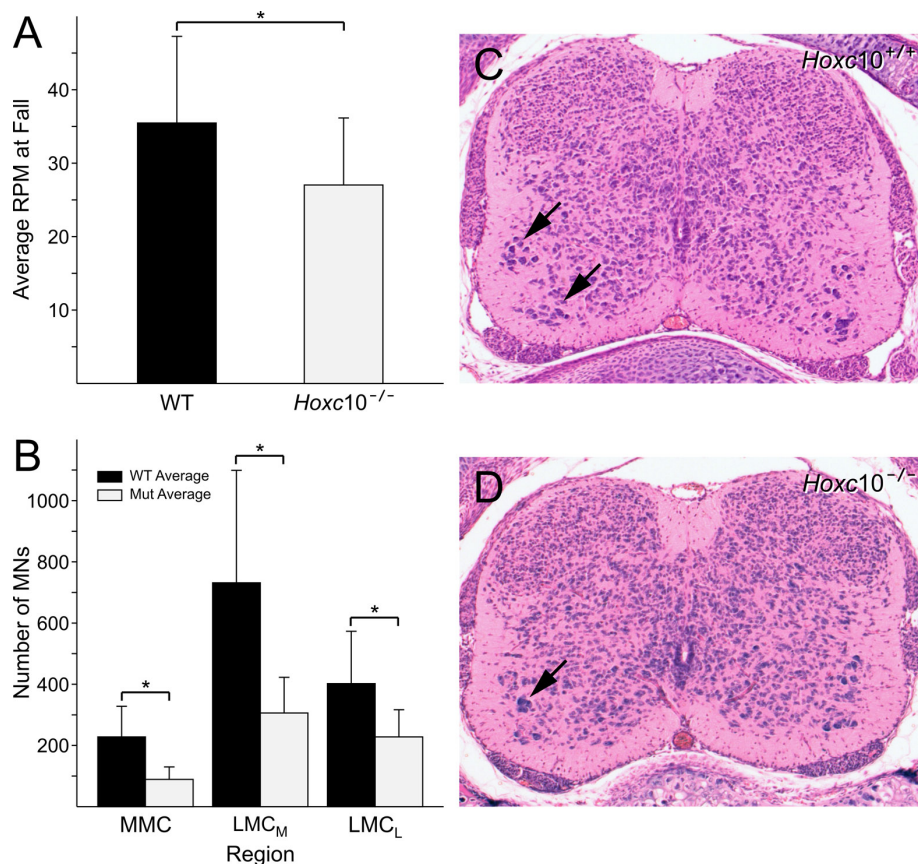


Figure 8: Rotarod behavior (A) and motor neuron cell counts (B) in *Hoxc10* mutants. (A) Mutant mice fall off the rotarod at lower RPMs than WT mice. Asterisk indicates a significance of $p < 0.001$ using a t-test comparison. (B) Decreases in lumbar motor neurons are seen in the medial motor column (MMC), and in the medial and lateral components of the lateral motor column (LMC_M and LMC_L) in *Hoxc10* mutant mice. Brackets and asterisks indicate a significance of $p < 0.05$ using t-test comparisons. C and D illustrate representative sections from *Hoxc10*^{+/+} and *Hoxc10*^{-/-} lumbar spinal cord used for motor neuron counting.

Discussion

Hoxa10, *Hoxc10*, and *Hoxd10* constitute a paralogous set of mammalian *Hox* genes. Previous studies have defined roles for *Hoxa10* and *Hoxd10* in patterning the axial and appendicular skeleton and the developing nervous system. Our current studies show that *Hoxc10* also participates in patterning these structures, supporting the idea that paralogous *Hox* genes may coordinately regulate the patterning and organization of a set of common structures. In developing embryos, *Hoxc10* is expressed in a broad posterior domain encompassing the developing neural tube and paraxial mesoderm. Expression is also evident in the developing kidney, genital tubercle, posterior mesenchyme, and surrounding cartilage condensations that form the pelvic bones. Like other *Abd-B*-related *Hox* genes, *Hoxc10* also expressed in the developing limb buds; however, unlike their paralogs and other *Abd-B*-related genes, *HoxC* expression is restricted to the developing hindlimb [21], in particular to perichondrium and ligaments in the proximal hindlimb. These areas of expression prefigure regions in which tissue alterations are observed in *Hoxc10* mutant mice. Alterations in axial and appendicular skeleton were observed, as were changes in nervous system structure and function.

Most *Hoxc10* mutant mice show a partial or complete absence of a rib on the 20th precaudal vertebrae. In C57Bl/6 mice, the 20th precaudal vertebra (PC20) is normally T13, the most caudal thoracic vertebra. The loss of the most caudal rib suggests a posterior transformation of the T13 vertebra to an L1 phenotype. As T9 exhibits the phenotype of transitional vertebra instead of T10, we can also conclude that the posterior transformation register extends anteriorly to at least T9. *Hoxa10* mutant mice often show a partial anterior transformation of the next most caudal thoracic vertebra, PC21, producing a partial rib and generating a T14 vertebra [8, 19]. Both PC20 and PC21 appear unaffected in *Hoxd10* mutant mice, however simultaneous inactivation of *Hoxa10* and *Hoxd10* commonly produces a complete anterior transformation of the PC21 to a full T14 phenotype [8]. Combinatorial inactivation of *Hoxa10* and *Hoxc10* also shows an anterior transformation including additional ribs and loss of lumbar and some sacral segments (Hostikka and Capecchi, unpublished observations). These combinatorial studies suggest that *Hoxa10* may be the dominant gene among the *Hox10* paralogues, as anterior transformations predominate in combinatorial mutants with *Hoxa10*, whereas *Hoxd10* and *Hoxc10* double mutants show a wide range of milder forms of intermediate lumbosacral

identities with the reoccurring theme of an expanded sacral domain (Hostikka and Capecchi, unpublished results). Thus, loss of activity of each of the three individual *Hox10* paralogues produces a different axial phenotype. The absence of all three *Hox10* genes produces mice with a transformation of all lumbar and sacral segments to a thoracic identity [16], further illustrating the requirement for *Hox10* paralogues in establishing lumbar skeletal identity. It should be noted that the *Hoxc10* allele used by Wellik and Capecchi is the allele described in this study, so allelic differences arising from *lacZ* fusion and the retention of *neo^R* in our construct are likely not a factor in producing axial skeletal phenotypes. The phenotypes observed in single and combinatorial mutations in the *Hox10* genes suggest a role for these three genes in establishing the division between thoracic, lumbar, and sacral vertebrae. Mutations in two of the three genes individually can alter the position of the boundary between regions by one segment anteriorly or posteriorly, while mutations in all three genes together serve to erase the boundary between regions entirely. These observations suggest a necessary balance in *Hox* gene activity, with activity of all three genes required to establish the correct rostrocaudal position of the lumbar vertebrae.

Another axial skeletal phenotype was observed in the formation of the pelvis, where evidence of dyssymphysis ischio-pubis was observed in all mutant animals. Dyssymphysis ischio-pubis has been reported as common, with 30-100% penetrance in several inbred strains by researchers in the 1940s - 1960s [10, 11, 31], however our wild-type siblings showed no evidence of this phenotype. Dyssymphysis ischio-pubis is erased in strain hybrids [31]; thus its absence in our wild-type controls could reflect some hybrid variability attributable to the small percentage of CC1.2 DNA carried in our parent lines. Alternatively, since the appearance of dyssymphysis ischio-pubis is tied to the presence of the *Hoxc10* mutation, this phenotype is likely attributable to the engineered mutation. Pelvic formation and placement appears otherwise unaffected.

Limb phenotypes include the presence of an abnormal branch of the iliofemoral ligament and remodeling of the femur to produce an ectopic anterior ridge and a modified profile in the shaft of the femur. Early muscle cleavage, and differentiation of the pelvic and hindlimb musculature occurs between embryonic day (E) 12.5 and E14.5, although the final muscle structure is not complete until after birth [32]. By E14.5 the femur has rotated anteromedially and projects ventrally rather than laterally from the acetabulum. During this process, the muscle anlagen

rotate with the femur and the ligament attachments to the pelvis form. In *Hoxc10* mutant mice, the femoral attachment extended minimally more anteriorly (or distally) than normal, with the femoral iliofemoral ligament attachment site broad enough to extend distally over the femoral growth plate during development, likely causing it to be torn into two branches by the growth of the femur. *Hoxc10* is highly expressed in the developing the ligaments as well as perichondrium of the attachment sites in the cartilage condensations of hip and femoral bones, and may be required for the maturation of the ligament, similar to suggested roles for *Hox* genes in cartilage differentiation and maturation [33, 34]. The absence of *Hoxa10* also leads to the production of an abnormal ligament [19], suggesting similar roles for other *Hox10* paralogues.

The presence of the ectopic femoral ridge in association with the abnormal iliofemoral ligament suggests a cause-and-effect relationship, whereby the ectopic ligament branch produces additional stresses on the developing femur. The adaptive response to these stresses is thus the formation of the ectopic ridge, similar to bony spurs. The bone formation likely appears through fibrocartilage calcification, but ligament attachment sites have also been suggested to function as growth plates [35, and references therein]. Femoral remodeling in response to load, compression and stress-shielding is seen throughout evolution [35, 36] and in the course of mammalian development. For example, femoral architecture shifts in humans in response to the transition to bipedal locomotion [37] and to changes in body mass [38]. The change in profile shape of the shaft of the femur also suggests altered stresses on the bone. The rounded profile and lack of a linea aspera in wild-type femurs suggests roughly equal forces applied via muscle attachments around the shaft of the femur, whereas, the triangular profile evident in mutant animals suggests a shift in the load-bearing of the femur, which would create novel strains on this bone, as the muscle attachment sites did not appear affected. However, as the heterozygotes show an intermediate phenotype, *Hoxc10* could be required for the periosteum to retain an oval shape against the stress of the attached muscles. The ability of the femur to undergo remodeling may also be affected by the differential production and placement of osteogenic cells. It has been suggested through archeological evidence that bone formation in stressed ligament attachment sites could be genetically dictated [35, and references therein]. Recently, the expression of *Hoxa2* has been shown to impair cartilage maturation [34] and our data could be interpreted as a premature maturation of cartilage

and osteogenic cells in the absence of *Hoxc10*. *Hoxc10* mice also appear more obese in adulthood than wild-type littermates. This extra weight may induce further stresses on the limb architecture, with concomitant changes in bone shape and structure, similar to remodeling events observed in obese humans [38].

Observations in *Hoxa10* and *Hoxd10* mutant mice have suggested that gene inactivation produces alterations in the placement and projection of lumbar motor neurons. *Hoxa10* mutants show anterior homeotic transformation of spinal nerves [4] while *Hoxd10* mutants have a reduced number of lumbar segments and shifts in the peripheral projections of spinal nerves [7]. Our observations in *Hoxc10* mice also suggest a nervous system phenotype, with mutant mice showing a significantly reduced number of lumbar motor neurons. The observed motor neuron loss is likely to contribute to the altered locomotor behavior observed in rotarod testing. *Hoxa10/Hoxd10* double mutant animals show significant reductions in the number of lumbar motor neurons, along with shifts in their position [9] and *Hoxc10/Hoxd10* double mutants show altered differentiation of rostral lumbar motor neurons, with a transformation of rostral lumbar motor neurons into a thoracic identity [20]. This combined set of observations suggests that *Hox10* gene expression has a significant role in patterning lumbar motor neurons.

In conclusion, our results provide evidence for a contribution of *Hoxc10* to the regulation of many aspects of body plan patterning. Significant changes are observed in both skeletal and nervous system patterning and the *Hoxc10* mouse appears to provide an excellent model for the study of mechanical stress on bone remodeling. Although deleting the entire *HoxC* complex appears to have negligible effects on embryonic patterning [39], the phenotype produced by selective deletion of *Hoxc10*, as well as other individual *HoxC* genes, demonstrates a clear dependence on the function of these genes to establish normal body plan development.

Supplementary Material

Supplemental figure 1

[<http://www.biolsci.org/v05p0397s1.pdf>]

Supplemental figure 2

[<http://www.biolsci.org/v05p0397s2.pdf>]

Acknowledgements

This study was supported by the Sigrid Juselius Foundation (SLH), the Finnish Cultural Foundation (SLH), and an NSF CAREER award to EMC. We wish to thank Mario Capecchi for support and encourage-

ment in the initial phases of this project and Derrick Rancourt for the CC1.2 specific genomic library.

Conflict of Interests

The authors have declared that no conflict of interest exists.

References

1. Scott MP. Vertebrate homeobox gene nomenclature. *Cell* 1992; 71: 551-553.
2. Duboule D. How to make a limb. *Science* 1996; 122: 449-460.
3. Davis AP, and Capecchi MR. Axial homeosis and appendicular skeleton defects in mice with a targeted disruption of *hoxd-11*. *Development* 1994; 120: 2187-2198
4. Rijli FM, Matyas R, Pellegrini M, et al. Cryptorchidism and homeotic transformations of spinal nerves and vertebrae in *Hoxa-10* mutant mice. *Proc Natl Acad Sci USA* 1995; 92: 8185-8189.
5. Satokata I, Bensen G, and Maas R. Sexually dimorphic sterility phenotypes in *Hoxa10*-deficient mice. *Nature* 1995; 374: 460-463.
6. Boulet AM and Capecchi MR. Targeted disruption of *hoxc-4* causes esophageal defects and vertebral transformations. *Dev Biol* 1996; 177: 232-249.
7. Carpenter EM, Goddard JM, Davis AP, et al. Targeted disruption of *Hoxd-10* affects mouse hindlimb development. *Development* 1997; 124: 4505-4514.
8. Wahba GM, Hostikka SL, and Carpenter EM. The paralogous *Hox* genes *Hoxa10* and *Hoxd10* interact to pattern the mouse hindlimb peripheral nervous system and skeleton. *Dev Bio.* 2001; 231: 87-102.
9. Lin A, and Carpenter EM. *Hoxa10* and *Hoxd10* coordinately regulate lumbar motor neuron patterning. *J Neurobiol* 2003; 56: 328-337.
10. Green EL. Genetic and non-genetic factors which influence the type of the skeleton in an inbred strain of mice. *Genetics* 1941; 26: 192-222.
11. McLaren A and Michie D. Factors affecting vertebral variation in mice. 1. Variation within inbred strain. *J Embryol Exp Morph.* 1954; 2: 149-160.
12. Burke AC, Nelson CE, Morgan BA, et al. *Hox* genes and the evolution of vertebrate axial morphology. *Development* 1995; 121: 333-346.
13. Wellik D. *Hox* patterning of the vertebrate axial skeleton. *Dev Dynamics* 2007; 236: 2454-2463.
14. Condie BG, and Capecchi MR. Mice with targeted disruptions in the paralogous genes *hoxa-3* and *hoxd-3* reveal synergistic interactions. *Nature* 1994; 370: 304-307.
15. Davis AP, Witte DP, Hsieh-Li HM, et al. Absence of radius and ulna in mice lacking *hoxa-11* and *hoxd-11*. *Nature* 1995; 375: 791-795.
16. Wellik D, and Capecchi MR. *Hox10* and *Hox11* genes are required to globally pattern the mammalian skeleton. *Science* 2003; 301: 363-367.
17. Carapuco M, Nóvoa A, Bobola N, et al. *Hox* genes specify vertebral types in the presomitic mesoderm. *Genes Dev.* 2005; 19: 2116-2121.
18. Benson GV, Lim H, Paria BC, et al. Mechanisms of reduced fertility in *Hoxa-10* mutant mice: uterine homeosis and loss of maternal *Hoxa-10* expression. *Development* 1996; 122: 2687-2696.
19. Favier B, Rijli FM, Fromental-Ramain C, et al. Functional cooperation between the non-paralogous genes *Hoxa-10* and *Hoxd-11* in the developing forelimb and axial skeleton. *Development* 1996; 122: 449-460.
20. Wu Y, Wang G, Scott SA, and Capecchi MR. *Hoxc10* and *Hoxd10* regulate mouse columnar, divisional and motor pool identity of lumbar motoneurons. *Development* 2007; 135: 171-182.
21. Hostikka SL, and Capecchi MR. The mouse *Hoxc11* gene: Genomic structure and expression pattern. *Mech Dev.* 1998; 70: 133-145.
22. Mansour, SL, Thomas, KR, Deng, CX, et al. Introduction of a lacZ reporter gene into the mouse int-2 locus by homologous recombination. *Proc Natl Acad Sci USA* 1990; 87: 7688-7692.
23. Deng CX, Thomas KR, and Capecchi MR. Location of cross-overs during gene targeting with insertion and replacement vectors. *Mol Cell Biol.* 1993; 13: 2134-2140.
24. Chisaka O, and Capecchi MR. Regionally restricted developmental defects resulting from targeted disruption of the mouse homeobox gene *hox-1.5*. *Nature* 1991; 350: 473-479.
25. Mansour, SL, Thomas, KR, and Capecchi, MR. Disruption of the proto-oncogene int-2 in mouse embryo-derived stem cells: a general strategy for targeting mutations to non-selectable genes. *Nature* 1988; 336: 348-352.
26. Choe A, Phun HQ, Tieu DD, et al. Expression patterns of *Hox10* paralogous genes during lumbar spinal cord development. *Gene Expr Patterns* 2006; 7: 730-737.
27. Carpenter EM, Goddard JM, Chisaka O, et al. Loss of *Hox-A1* (*hox-1.6*) function results in the reorganization of the murine hindbrain. *Development* 1993; 118: 1063-1075.
28. Pollock RA, Jay G, and Bieberich CJ. Altering the boundaries of *Hox3.1* expression: evidence for antipodal gene regulation. *Cell* 1992; 71: 911-923.
29. Gruneberg H. Genetical studies on the skeleton of the mouse. IV. Quasi-continuous variations. *J Genetics* 1952; 51: 95-114.
30. Stein KF. Genetical studies on the skeleton of the mouse. XXI The girdles and the long bones. *J Genet* 1957; 55: 313-324.
31. Howe WL, and Parsons PA. Genotype and environment in the determination of minor skeletal variants and body weight in mice. *J Embryol exp Morph* 1967; 17: 293-292.
32. Lance-Jones C. The morphogenesis of the thigh of the mouse with special reference to tetrapod muscle homologies. *J Morph* 1979; 162: 275-310.
33. Yueh YG, Gardner DP, and Kappen C. Evidence for regulation of cartilage differentiation by the homeobox gene *Hoxc8*. *Proc Natl Acad Sci USA* 1998; 95: 9956-9961.
34. Massip L, Ectors F, Deprez P, et al. Expression of *Hoxa2* in cells entering chondrogenesis impairs overall cartilage development. *Differentiation* 2007; 75: 256-267.
35. Benjamin M, Toumi H, Ralphs JR, et al. Where tendons and ligaments meet bone: attachment sites ('enthesis') in relation to exercise and/or mechanical load. *J Anat* 2006; 208: 471-490.
36. Martin RB. Functional adaptation and fragility of the skeleton. In: Agarwal SC., and Stout SD, eds. *Bone Loss and Osteoporosis: An Anthropological Perspective*. New York: Kluwer Academic/Plenum Publishers. 2003: 121-138.
37. Ryan TM, and Krovitz GE. Trabecular bone ontogeny in the human proximal femur. *J Hum Evol* 2006; 51: 591-602.
38. Ruff CB, Scott WW, and Liu AY. Articular and diaphyseal remodeling of the proximal femur with changes in body mass in adults. *Am J Phys Anthropol* 1991; 86: 397-413.
39. Suemori H, and Noguchi S. *Hox C* cluster genes are dispensable for overall body plan of mouse embryonic development. *Dev Biol* 2000; 220: 333-342.